DOI: 10.1002/ange.201409216

Self-Assembly

Geometrically Restricted Intermediates in the Self-Assembly of an $M_{12}L_{24}$ Cuboctahedral Complex[**]

Daishi Fujita, Hiroyuki Yokoyama, Yoshihiro Ueda, Sota Sato, and Makoto Fujita[*]

Abstract: *The self-assembly of a cuboctahedral $M_{12}L_{24}$ complex is traced by time-dependent NMR spectroscopy and mass spectrometry. The metastable intermediate structures that exist during the self-assembly process are not a chaotic mixture of numerous species, but instead are geometrically restricted. Short-lived M_8L_{16} (D_{4d}) and relatively long-lived M_9L_{18} (D_{3h}) are fully characterized as major intermediates. Employing a ligand with a smaller bend angle (112°) allows these two species to be kinetically trapped and more clearly observed by NMR spectroscopy. X-ray crystallography shows that M_9L_{18} has the framework topology predicted by geometric discussion.*

Self-assembly of Platonic and Archimedean solids from metal and small-ligand components is currently a topic of considerable interest.[1–3] Using only simple procedures, the components spontaneously find the right pathways that lead to stable polyhedral structures. In most cases, only these resultant stable polyhedral structures are characterized and thoroughly discussed, and far less attention has been paid to the metastable intermediate structures that exist during the self-assembly process.[4] This is, in part, due to the difficulties in characterizing such transient, short-lived species, but also largely due to the prejudice that a number of intermediates/pathways exist before the assembly process reaches the final stable structures.[5]

The polyhedral structures are, however, formed under a geometrical restriction known as Euler's polyhedron theorem. We assumed that this geometrical restriction would also apply to the intermediates of self-assembly, thus limiting the number of metastable intermediate structures and self-assembly pathways. Accordingly, the self-assembly of $M_{12}L_{24}$ complex **2** from Pd^{II} ions and bent ligand **1** was carefully traced by time-dependent NMR spectroscopy and mass spectrometry. Surprisingly, both analyses consistently revealed the formation of just two intermediate species: first the short-lived M_8L_{16} and then the relatively long-lived M_9L_{18}. No other species were identified as intermediates before the assembly process reached the final $M_{12}L_{24}$ complex. Our results thus demonstrate that the geometrical restraints even apply to the intermediates of self-assembly, and facilitate the self-assembly of giant polyhedra. By using a ligand with a reduced bend angle (112°), the M_9L_{18} intermediate was directly crystallized, and crystallographic analysis showed that the structure has the predicted framework topology.

To access the self-assembly intermediates, we synthesized new $M_{12}L_{24}$ precursor ligand **1**, which incorporates a triazine core with a 2-methyl substituent as a probe for NMR studies. We first confirmed that ligand **1** self-assembled into $M_{12}L_{24}$ spherical complex **2** by using the reported procedure.[6] Ligand **1** (14.7 μmol) was treated with $Pd(NO_3)_2$ (11.7 μmol) and stirred for three days at 80 °C in [D$_6$]DMSO. The ^{1}H NMR measurement gave a simple spectrum with downfield shifting of the pyridine peaks and line broadening (Figure 1 b) that are characteristic of $M_{12}L_{24}$ assemblies.[6] A single diffusion band in the ^{1}H diffusion-ordered NMR spectroscopy (DOSY; see Figure S6 in the Supporting Information, SI) and a series of $[Pd_{12}L_{24}(BF_4)_{24-n}]^{n+}$ ion peaks in the cold-spray ionization mass spectrometry (CSI-MS)[7] (Figure 2 a) analyses supported the exclusive formation of **2**. X-ray crystallographic analysis of a single crystal grown from the DMSO solution confirmed the formation of **2**, which has cuboctahedral symmetry (Figure 1 d).

We then set out to examine the self-assembly intermediates that exist prior to complete convergence to the thermodynamically stable $M_{12}L_{24}$ structure. ^{1}H NMR spectra of a nonheated (rt, 30 min) mixture of ligand **1** and $Pd(NO_3)_2$ showed, in addition to the known $M_{12}L_{24}$ peaks, other noticeable signals (Figure 1 c), which are presumably derived from metastable intermediates. An important clue was obtained from careful CSI-MS analysis. Comparison of the spectra of the converged $M_{12}L_{24}$ and the nonconverged self-assembly mixtures showed two distinct series of ions that were only observed in the nonconverged spectrum (Figure 2 a,b). By MS analysis at high resolution, these two ion series were reliably assigned to $[Pd_8L_{16}(BF_4)_{16-n}]^{n+}$ ($n = 8$–11) and $[Pd_9L_{18}(BF_4)_{18-n}]^{n+}$ ($n = 8$–12), respectively. The isotopic distribution patterns of each peak clearly match the simulated patterns (Figures S10–S15).

To verify that these Pd_8L_{16} and Pd_9L_{18} species are trapped as metastable intermediates rather than as side products, we examined whether Pd_8L_{16} and Pd_9L_{18} would spontaneously convert to the stable $Pd_{12}L_{24}$ upon heating. Figure 2 c,d shows magnified views of representative peaks assigned to Pd_8L_{16} (11+) and Pd_9L_{18} (11+). We observed that Pd_8L_{16} disappeared selectively over Pd_9L_{18} after heating for 1 h at 60 °C.

---

[*] Dr. D. Fujita, H. Yokoyama, Dr. Y. Ueda, Dr. S. Sato,
Prof. Dr. M. Fujita
Department of Applied Chemistry, Graduate School of Engineering
The University of Tokyo
7-3-1 Hongo, Bunkyo-ku, Tokyo 113-8656 (Japan)
E-mail: mfujita@appchem.t.u-tokyo.ac.jp

[**] This work was supported by the Japanese Ministry of Education, Culture, Sports, Science, and Technology (MEXT) with their Grant-in-Aids for Scientific Research on Innovative Areas (25102007) and for Young Scientists (A) (24685010). The synchrotron X-ray crystallography was performed at the BL1A beamline at the KEK Photon Factory (2011G522) and at the BL41XU beamline at SPring-8 (2014A0042).

Supporting information for this article is available on the WWW under http://dx.doi.org/10.1002/anie.201409216.

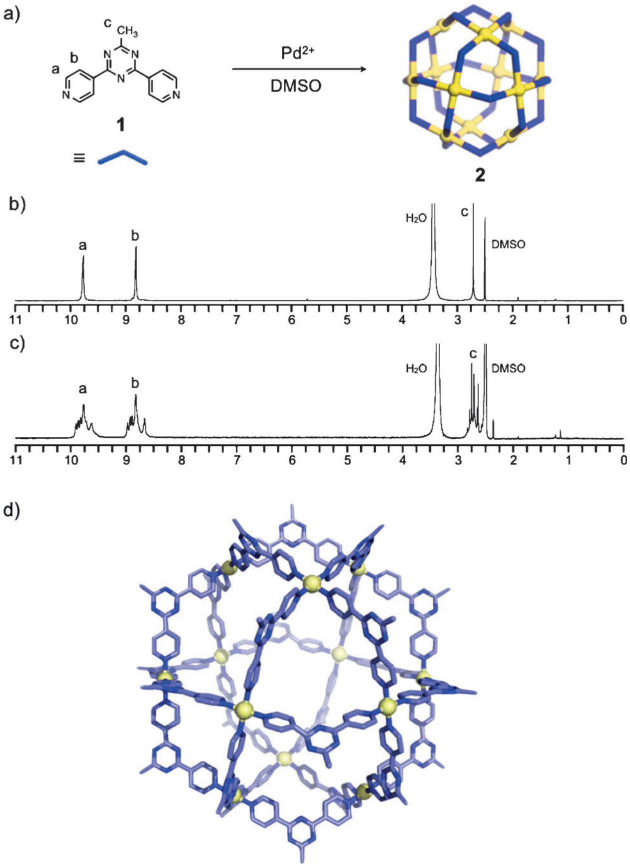

Figure 1. a) Schematic representation of the self-assembly of $M_{12}L_{24}$ complex **2**. b,c) ^1H NMR spectra (500 MHz, [D$_6$]DMSO, 300 K) after mixing ligand **1** and Pd^{II} at b) 80 °C for 3 d, and c) rt for 30 min. d) X-ray crystal structure of **2** (BF_4^- salt). Hydrogen atoms, counter ions, and solvent molecules have been omitted for clarity.

Additional heating for 6 h at 80 °C caused the remaining Pd_9L_{18} species to disappear as well. The comprehensive time-dependent behavior in the CSI-MS study (see Section 3.1 of SI) demonstrates the existence of short-lived Pd_8L_{16} and relatively long-lived Pd_9L_{18} as metastable intermediates in the formation of $Pd_{12}L_{24}$.

The framework topologies of Pd_8L_{16} and Pd_9L_{18} intermediates could be predicted by mathematical discussion. Under the postulate that each vertex (M) connects four edges (L), the possible polyhedral topologies for M_8L_{16} and M_9L_{18} are limited to one each. Figure 3 shows models of these unique topologies, **3** for M_8L_{16} (D_{4d}) and **4** for M_9L_{18} (D_{3h}), which do not express any significant distortion. Interestingly, no allowed structures exist for M_nL_{2n}, in which $n \leq 5$ and $n = 7$. A possible structure for $n = 6$ is unrealistically distorted as our ligand bend angle is much larger than the ideal 90° required for the $n = 6$ structure. $M_{10}L_{20}$ and $M_{11}L_{22}$ are geometrically allowed but already very close to the final $M_{12}L_{24}$. Thus, they may exist as momentary, unobservable intermediates. All the possible topologies for M_nL_{2n} ($n < 12$) are summarized in Figure S23.

Based on both the experimental and theoretical discussions, we went over the ^1H NMR experiments to confirm the intermediate structures. Both **3** and **4** have two different ligand environments, illustrated by red and blue edges in Figure 3. The ratios of the two ligands are 1:1 for **3** (D_{4d}) and 2:1 for **4** (D_{3h}), respectively. These environmental differences were clearly distinguishable from the signals of the methyl

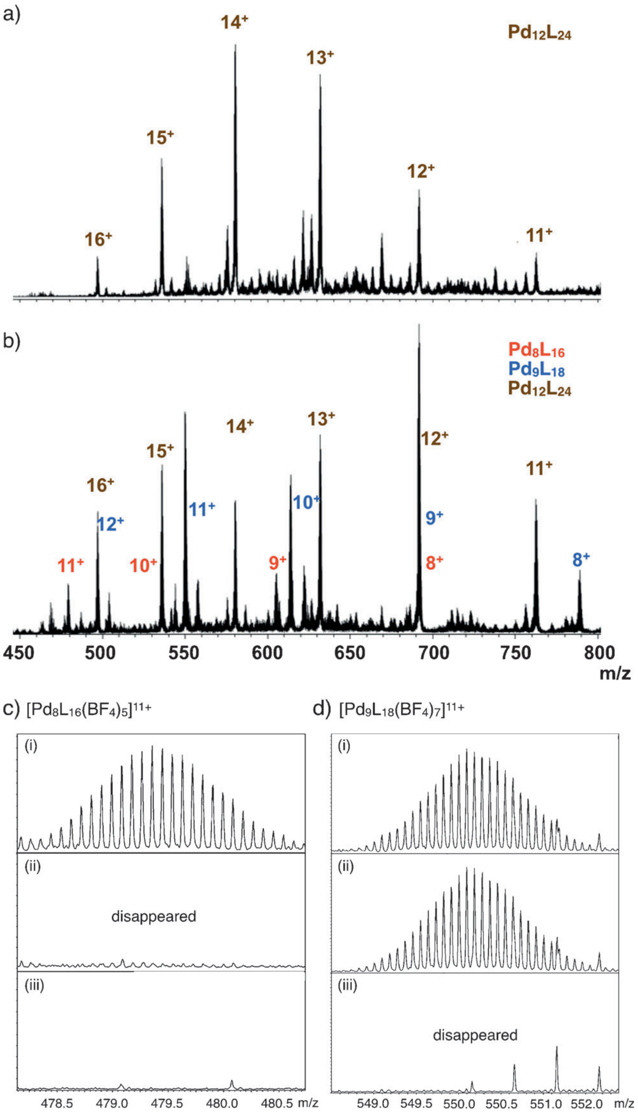

Figure 2. CSI-TOF mass spectra of ligand **1** and Pd^{II} (BF_4^- salt) under different self-assembly conditions: a) 80 °C, 6 h. b) rt, 30 min. c,d) Comparison of expanded spectra of c) the 11+ peak of Pd_8L_{16} ([$Pd_8L_{16}(BF_4)_5$]$^{11+}$) and d) the 11+ peak of Pd_9L_{18} ([$Pd_9L_{18}(BF_4)_7$]$^{11+}$) after 30 min at rt (i), 1 h at 60 °C (ii), and 6 h at 80 °C (iii).

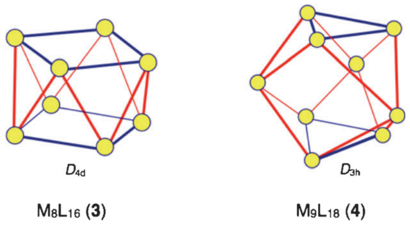

Figure 3. Geometrically allowed topologies for M_8L_{16} and M_9L_{18} compositions with D_{4d} and D_{3h} symmetries, respectively. Both M_8L_{16} and M_9L_{18} have two edge environments (colored in red and blue).

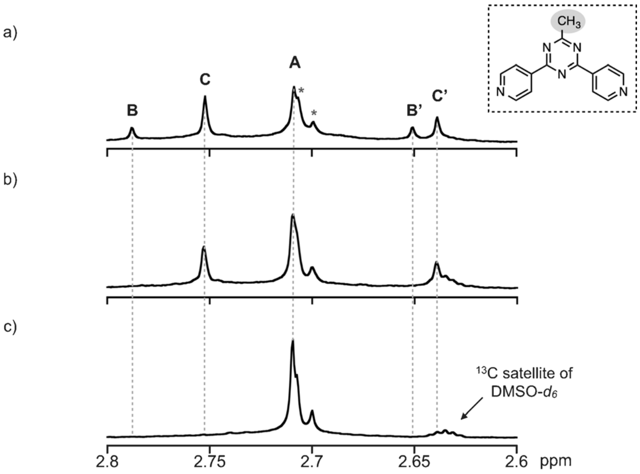

Figure 4. Time-dependent ^{1}H NMR spectra (500 MHz, [D$_6$]DMSO, 300 K) for the self-assembly of ligand **1** and Pd^{II}: a) rt, 30 min, b) 60 °C, 1 h, and c) 80 °C, 6 h. The peak labeled A corresponds to the methyl protons of $Pd_{12}L_{24}$. Pairs of B, B′ (1:1) and C, C′ (2:1) are assigned to Pd_8L_{16} and Pd_9L_{18}, respectively. Unassignable minor peaks were detected at 2.57, 2.70, 2.71, and 2.83 ppm.

probe on ligand **1** (Figure 4). The single peak **A** was assigned to **2**, whereas peaks **B** and **B**′ were assigned to **3** and peaks **C** and **C’** to **4**. The ratio of **B** and **B**′ is 1:1, and that of **C** and **C’** is 2:1; this is in good agreement with the topologies and symmetries of **3** and **4**, respectively. Peaks **B** and **B**′ disappeared after heating for 1 h at 60 °C, and peaks **C** and **C’** subsequently disappeared upon additional heating for 6 h at 80 °C, which is fully consistent with the time-dependent MS study.

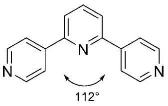

5

When ligand **5** with a smaller bend angle (112°) was employed, its M_8L_{16} and M_9L_{18} complexes, **6** and **7**, were kinetically trapped because their framework distortions are considerably reduced. Complexation at 80 °C for 14 h afforded a mixture of **6** and **7**, from which **7** was isolated as single crystals. The crystal structure confirmed the predicted D_{3h} framework of **7** (Figure 5). The sum of the *cis*-N-Pd-N angles at every Pd^{II} ion is close to 360° (359.8°–360.1°), which indicates that there are no distortions around any of the Pd^{II} centers.

In summary, we have designed and performed experiments to uncover self-assembly intermediates that exist in the course of the formation of an $M_{12}L_{24}$ cuboctahedral complex. The time-dependent NMR and CSI-MS analyses consistently showed the exclusive formation of just two metastable intermediates: M_8L_{16} and M_9L_{18}. This suggests that the geometrical restriction begins from the early stages of the self-assembly process, and may serve to guide the self-assembly into the final giant polyhedral structures. The framework topology of the intermediates was mathematically predicted. This newly disclosed self-assembly pathway is reminiscent of the folding funnel hypothesis for protein folding,[8] in which proteins drop down to their ground state guided by a number of trappings in local minima along the way.

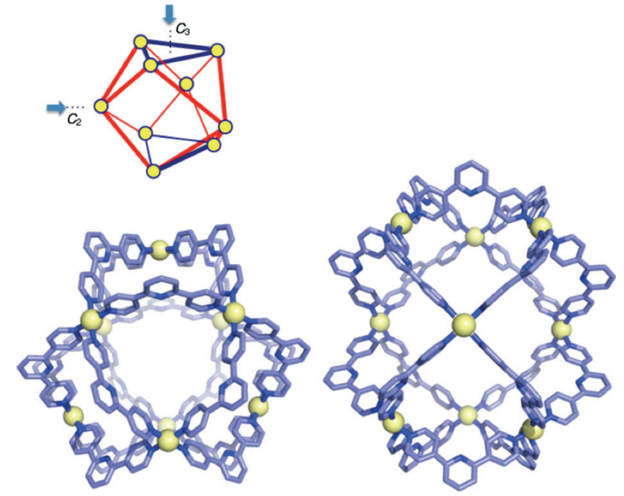

Figure 5. X-ray crystal structure of Pd_9L_{18} complex **7**. View along the C3 (left) and C2 (right) axes. Hydrogen atoms and counter ions (BF_4^-) have been omitted for clarity. Crystal data: space group $P2_1/m$, $a = 53.598(11)$ Å, $b = 43.824(9)$ Å, $c = 53.599(11)$ Å, $\beta = 120.01(3)°$, $V = 109022(38)$ Å^3, $Z = 6$, $R_1 = 0.1244$, $wR2 = 0.3667$, GOF = 1.177.

Experimental Section

Preparation of $M_{12}L_{24}$ complexes **2**: Ligand **1** (14.7 μmol) was treated with $Pd(NO_3)_2$ or $Pd(BF_4)_2{\cdot}(CH_3CN)_4$ (11.7 μmol) in DMSO (0.74 mL) at 80 °C for 3 d. ^{1}H NMR spectroscopy confirmed the quantitative formation of $M_{12}L_{24}$ spherical complex **2**. ^{1}H NMR (500 MHz, [D$_6$]DMSO, 300 K, NO_3^- salt) $\delta = 9.77$ (br, 96 H), 8.81 (br, 96 H), 2.71 ppm (br, 72 H). Diffusion coefficient ([D$_6$]DMSO, 300 K, NO_3^- salt): $D = 5.0 \times 10^{-11}$ m^{2}s^{-1}. ^{13}C NMR (150 MHz, [D$_6$]DMSO, 300 K, BF_4^- salt) $\delta = 179.3$ (C), 168.3 (C), 152.8 (CH), 146.1 (C), 126.1 (CH), 26.2 ppm (CH$_3$). The following signals are the signals with the highest intensity among the isotope patterns of each ion peak. *m*/*z* calcd for $[M-14(BF_4^-)]^{14+}$ 580.5945, found 580.5942; calcd for $[M-13(BF_4^-)]^{13+}$ 631.8714, found 631.8708; calcd for $[M-12(BF_4^-)]^{12+}$ 691.7777, found 691.7774; calcd for $[M-11(BF_4^-)]^{11+}$ 762.4851, found 762.4844; calcd for $[M-10(BF_4^-)]^{10+}$ 847.4340, found 847.4339; calcd for $[M-9(BF_4^-)]^{9+}$ 951.3717, found 951.3718; calcd for $[M-8(BF_4^-)]^{8+}$ 1081.0437, found 1081.0453; calcd for $[M-7(BF_4^-)]^{7+}$ 1247.9076, found 1247.9085.

Received: September 17, 2014

Keywords: geometrical restriction · metastable intermediates · palladium · self-assembly

---

[1] Earlier examples: a) M. Fujita, D. Oguro, M. Miyazawa, H. Oka, K. Yamaguchi, K. Ogura, *Nature* **1995**, *378*, 469–471; b) D. L. Caulder, R. E. Powers, T. N. Parac, K. N. Raymond, *Angew. Chem. Int. Ed.* **1998**, *37*, 1840–1842; *Angew. Chem.* **1998**, *110*, 1940–1943; c) B. F. Abrahams, S. J. Egan, R. Robson, *J. Am. Chem. Soc.* **1999**, *121*, 3535–3536; d) A. Müller, V. P. Fedin, C. Kuhlmann, H. Bçgge, M. Schmidtmann, *Chem. Commun.* **1999**, 927–928; e) B. Olenyuk, M. D. Levin, J. A. Whiteford, J. E. Shield, P. J. Stang, *Nature* **1999**, *398*, 796–799; f) M. Ni, A. Tassar, T. Antoun, O. M. Yaghi, *J. Am. Chem. Soc.* **2005**, *127*, 12752–12753.

[2] Recent examples: a) M. Liu, W. Liao, C. Hu, S. Du, H. Zhang, *Angew. Chem. Int. Ed.* **2012**, *51*, 1585–1588; *Angew. Chem.* **2012**, *124*, 1617–1620; b) A, Stephenson, D. Sykes, M. D. Ward,

Dalton Trans. **2013**, *42*, 6756–6767; c) Q. F. Sun, S. Sato, M. Fujita, *Nat. Chem.* **2012**, *4*, 330–333; d) K. Xiong, F. Jiang, Y. Gai, D. Yuan, L. Chen, M. Wu, K. Su, M. Hong, *Chem. Sci.* **2012**, *3*, 2321–2325; e) R. A. Bilbeisi, J. K. Clegg, N. Elgrishi, X. d. Hatten, M. Devillard, B. Breiner, P. Mal, J. R. Nitschke, *J. Am. Chem. Soc.* **2012**, *134*, 5110–5119; f) M. Otte, P. F. Kuijpers, O. Troeppner, I. Ivanović-Burmazović, J. N. H. Reek, B. d. Bruin, *Chem. Eur. J.* **2013**, *19*, 10170–10178; g) S. Pasquale, S. Sattin, E. C. Escudero-Adan, M. Martinez-Belmonte, J. d. Mendoza, *Nat. Commun.* **2012**, *3*, 785; h) Q. F. Sun, J. Iwasa, D. Ogawa, Y. Ishido, S. Sato, T. Ozeki, Y. Sei, K. Yamaguchi, M. Fujita, *Science* **2010**, *328*, 1144–1147; i) D. Fujita, K. Suzuki, S. Sato, M. Yagi-Utsumi, Y. Yamaguchi, N. Mizuno, T. Kumasaka, M. Takata, M. Noda, S. Uchiyama, K. Kato, M. Fujita, *Nat. Commun.* **2012**, *3*, 1093.

[3] Reviews: a) M. Han, D. M. Engelhard, G. H. Clever, *Chem. Soc. Rev.* **2014**, *43*, 1848–1860; b) M. M. J. Smulders, I. A. Riddell, C. Browne, J. R. Nitschke, *Chem. Soc. Rev.* **2013**, *42*, 1728–1754; c) K. Harris, D. Fujita, M, Fujita, *Chem. Commun.* **2013**, *49*, 6703–6712; d) T. R. Cook, Y. R. Zheng, P. J. Stang, *Chem. Rev.* **2013**, *113*, 734–777; e) A. Müller, P. Kçgerler, A. W. M. Dress, *Coord. Chem. Rev.* **2001**, *222*, 193–218; f) D. L. Caulder, K. N. Raymond, *Acc. Chem. Res.* **1999**, *32*, 975–982.

[4] a) A. V. Davis, R. M. Yeh, K. N. Raymond, *Proc. Natl. Acad. Sci. USA* **2002**, *99*, 4793–4796; b) J. M. Lehn, *Proc. Natl. Acad. Sci. USA* **2002**, *99*, 4763–4768; c) J. M. Lehn, *Chem. Soc. Rev.* **2007**, *36*, 151–160.

[5] a) M. D. Levin, P. J. Stang, *J. Am. Chem. Soc.* **2000**, *122*, 7428–7429; b) N. Fatin-Rouge, S. Blanc, A. Pfeil, A. Rigault, A.-M. Albrecht-Gray, J.-M. Lehn, *Helv. Chim. Acta* **2001**, *84*, 1694–1711; c) S. Sato, Y. Ishido, M. Fujita, *J. Am. Chem. Soc.* **2009**, *131*, 6064–6065; d) H. N. Miras, G. J. T. Cooper, D.-T. Long, H. Bögge, A. Müller, C. Streb, L. Cronin, *Science* **2010**, *327*, 72–74; e) J. J. Pak, J. Greaves, D. J. McCord, K. Shea, *Organometallics* **2002**, *21*, 3552–3561; f) Y.-R. Zheng, P. J. Stang, *J. Am. Chem. Soc.* **2009**, *131*, 3487–3489; g) V. M. Cangelosi, T. G. Carter, L. N. Zakharov, D. W. Johnson, *Chem. Commun.* **2009**, 5606–5608; h) A. Marquis, J. Kintzinger, R. Graff, P. N. Baxter, J.-M. Lehn, *Angew. Chem. Int. Ed.* **2002**, *41*, 2760–2764; *Angew. Chem.* **2002**, *114*, 2884–2888; i) S. J. Dalgarno, N. P. Power, J. E. Warren, J. L. Atwood, *Chem. Commun.* **2008**, 1539–1541; j) W. Jiang, A. Schäfer, P. C. Mohr, C. A. Schalley, *J. Am. Chem. Soc.* **2010**, *132*, 2309–2320; k) N. Fatin-Rouge, S. Blanc, E. Leize, A. Van Dorsselaer, P. Baret, J. L. Pierre, A. M. Albrecht-Gary, *Inorg. Chem.* **2000**, *39*, 5771–5778; l) M. Elhabiri, J. Hamacek, J. C. G. Bunzli, A. M. Albrecht-Gary, *Eur. J. Inorg. Chem.* **2004**, 51–62; m) B. Hasenknopf, J. M. Lehn, N. Boumediene, E. Leize, A. Van Dorsselaer, *Angew. Chem. Int. Ed.* **1998**, *37*, 3265–3268; *Angew. Chem.* **1998**, *110*, 3458–3460; n) M. Albrecht, S. Dehn, R. Frohlich, *Angew. Chem. Int. Ed.* **2006**, *45*, 2792–2794; *Angew. Chem.* **2006**, *118*, 2858–2860; o) C. Su, Y. Cai, C. Chen, F. Lissner, B. Kang, W. Kaim, *Angew. Chem. Int. Ed.* **2002**, *41*, 3371–3375; *Angew. Chem.* **2002**, *114*, 3519–3523; p) J. A. Sheikh, H. S. Jena, A. Adhikary, S. Khatua, S. Konar, *Inorg. Chem.* **2013**, *52*, 9717–9719; q) C. G. Claessens, M. J. Vicente-Aranab, T. Torres, *Chem. Commun.* **2008**, 6378–6380; r) Y. Tsujimoto, T. Kojima, Shuichi Hiraoka, *Chem. Sci.* **2014**, *5*, 4167–4172; s) M. Yoneya, T. Yamaguchi, S. Sato, M. Fujita, *J. Am. Chem. Soc.* **2012**, *134*, 14401–14401.

[6] M. Tominaga, K. Suzuki, M. Kawano, T. Kusukawa, T. Ozeki, S. Sakamoto, K. Yamaguchi, M. Fujita, *Angew. Chem. Int. Ed.* **2004**, *43*, 5621–5625; *Angew. Chem.* **2004**, *116*, 5739–5743.

[7] a) S. Sakamoto, M. Fujita, K. Kim, K. Yamaguchi, *Tetrahedron* **2000**, *56*, 955–964; b) K. Yamaguchi, *J. Mass Spectrom.* **2003**, *38*, 473–490.

[8] R. H. Pain, *Mechanisms of Protein Folding, 2nd ed.*, Oxford University Press, Oxford, **2000**.